Identification and functional characterization of the astacidin family of proline-rich host defence peptides (PcAst) from the red swamp crayfish (Procambarus clarkii, Girard 1852)

Identification and functional characterization of the astacidin family of proline-rich host defence peptides (PcAst) from the red swamp crayfish (*Procambarus clarkii,* Girard 1852)

Tomislav Rončević[a,b], Vedrana Čikeš-Čulić[c], Ana Maravić[d], Francesca Capanni[e], Marco Gerdol[e], Sabrina Pacor[e], Alessandro Tossi[e], Piero G. Giulianini[e], Alberto Pallavicini[e], Chiara Manfrin[e,*]

[a] *Department of Biology, Faculty of Science, University of Split, Rudera Boskovica 33, 21000, Split, Croatia*
[b] *Institute of Oceanography and Fisheries, Setaliste Ivana Mestrovica 63, 21000, Split, Croatia*
[c] *Department of Medical Chemistry and Biochemistry, School of Medicine, University of Split, Soltanska 2, 21000, Split, Croatia*
[d] *Department of Biology, Faculty of Science, University of Split, Rudera Boskovica 33, 21000, Split, Croatia*
[e] *Department of Life Sciences, University of Trieste, via L. Giorgieri, 5, IT-34127, Trieste, Italy*

ARTICLE INFO

Keywords:
Procambarus clarkii
Immunity
Astacidin
Antimicrobial peptide
Transcriptome
Crayfish

ABSTRACT

This study reports the identification of four novel proline-rich antimicrobial peptides (PR-AMP) from the transcriptome of the red swamp crayfish *Procambarus clarkii*. The newly identified putative peptides (PcAst-1b, -1c, −2 and −3), which are related with the previously identified hemocyte-specific PR-AMP astacidin-1, are encoded by the multi-genic astacidin gene family. The screening of available and proprietary transcriptomes allowed to define the taxonomical range of distribution of this gene family to Astacoidea and Parastacoidea. The antimicrobial properties of three synthetic PcAst peptides (PcAst-1a, -1b/c and −2), were characterized against reference bacteria or multidrug resistant clinical isolates, and their cytotoxicity was evaluated towards human transformed cell lines. The antimicrobial activity ranged from potent and broad-spectrum, in low-salt medium, to poor, whereas it was generally low in full nutrient broth. No significant toxic effects were observed on cultured human cells. RNA-seq data from 12 different tissues indicated a strong specificity for haemocytes under naïve physiological condition, with moderate expression (5-fold lower) in gills. Quantitative real time PCR revealed a rapid (within 2 h) and significant up-regulation of PcAst-1a (Astacidin 1) and PcAst-2 expression in response to LPS injection. Due to the variation in antimicrobial potency and inducibility, the roles of the other astacidins (PcAst-1b, -1c and −3) need to be further investigated to determine their significance to the immune responses of the red swamp crayfish.

1. Introduction

Phagocytosis, encapsulation and melanisation are key innate immune responses that invertebrates enact against pathogen infections (Jiravanichpaisal et al., 2010; Liu et al., 2007). Crustaceans are one of the most abundant and diverse group of metazoans and, due to their colonization of widely different environments, they are considered an important source of bioactive molecules (Zhu et al., 2019). In particular, the lack of an adaptive immune system has led to the evolution of effective antibiotic molecules, including different types of antimicrobial peptides (AMPs). These molecules can be highly diverse in their primary structure, but they generally share a cationic nature and common structural features such as an amphipathic residue arrangement, as well as functional characteristics such as inducibility following exposure of the organism to pathogen associated molecular patterns (PAMPs) (Ganz and Lehrer, 1994; Hancock and Diamond, 2000). In fact, AMPs are recognised as important components of the innate immune system, nearly universally present in multicellular organisms (Hoffmann et al., 1999; Jiravanichpaisal et al., 2010; Zasloff, 2002).

Invertebrate AMPs are commonly grouped into three families, based on some common structural features: *i)* cysteine-free, linear peptides that adopt an amphipathic, alpha-helical structure and generally have a membranolytic mode-of-action (well-known examples are insect cecropins) (Steiner et al., 1981), *ii)* peptides with two or more cysteine

Abbreviations: DiOC6, 3.3′-dihexyloxacarbocyanine iodide; DOPC, 1.2-dioleoyl-sn-glycero-3-phosphocholine DOPC; MTT, 3-(4.5-dimethylthiazol-2-yl)-2.5-diphenyl tetrazolium bromide; PI, propidium iodide; PG, phosphatidylglycerol; LPS, Lipopolysaccharide; cDNA, complementary DNA; PAMP, pathogen-associated molecular patterns

* Corresponding author.
E-mail address: cmanfrin@units.it (C. Manfrin).

residues forming disulfide bridged, β-sheet structures (e.g. defensins) (Kagan et al., 1994), and *iii)* linear peptides with an overrepresentation of proline and/or glycine residues, which may or may not have disulphide-stabilized structures (Otvos, 2002).

The first AMP to be partially characterized in crustaceans was a peptide pertaining to the third type, isolated from the haemolymph of the shore crab *Carcinus maenas*; a 6.5 kDa proline-rich peptide (Schnapp et al., 1996) and other similar peptides have been recently reported from three species of mud crabs (Imjongjirak et al., 2017). This original report was shortly followed by the identification of penaeidins, a family of proline-rich AMPs that also contain a C-terminal, Cys-rich domain (Cuthbertson et al., 2008; Destoumieux et al., 1997; Wu et al., 2019). These AMPs, found in shrimps and prawns of the *Penaeus* genus, are active against both Gram-negative and Gram-positive bacteria. The first evidence of proline-rich AMPs in crayfish dates to 2007 (Jiravanichpaisal et al., 2007), when astacidin 2 was characterized from the plasma of *Pacifastacus leniusculus*. This AMP is relatively short (14–16 aa in length) and shows a broad range of antibacterial activity, inhibiting the growth of both Gram-positive and -negative bacteria.

The red swamp crayfish, *Procambarus clarkii*, is widely distributed in natural environments (Lodge et al., 2012), and it is also a cultured species worldwide (Gong et al., 2012; Jin et al., 2019). Due to its economic importance for aquaculture, its immune system has been extensively studied (Dai et al., 2017; Du et al., 2016; Wu et al., 2017; Zhou et al., 2017). However, only a single 20 aa-long astacidin, highly similar to *P. leniusculus* astacidin 2 and mainly expressed in haemocytes and gills, has been identified so far (Shi et al., 2014) in this species.

Here we report the identification of four potential transcripts pertaining to the proline-rich astacidin family in *P. clarkii*, thanks to a whole-transcriptome sequencing approach. The functional characterisation of these peptides, together with the elucidation of their molecular diversity, evolutionary history, constitutive expression in different tissues and inducibility after LPS-challenge, allowed to shed some light on their possible role in crayfish immunity.

2. Materials and methods

2.1. Peptide identification

The identification of novel astacidin peptides followed a robust procedure based on the use of conserved signal peptides, similar to that previously reported for identifying AMPs in placozoa and teleost fish (Simunić et al., 2014; Tessera et al., 2012), since these are known to be generally well conserved to allow the efficient secretion of defence peptides. Briefly, the signal sequence (MRLLYLLGVVLVALMAAVPSQA) from *Pacifastacus leniusculus* astacidin (UniProt entry Q0PJU7) (Jiravanichpaisal et al., 2007) was identified using SignalP 4.1 (Petersen et al., 2011), and used to query available *Procambarus clarkii* transcriptomic resources for transcripts encoding sequences related to AMPs with TBLASTN. These resources included the dbEST database (Boguski et al., 1993) as well as a comprehensive transcriptome assembly (hereafter defined ATLAS) deriving from 12 different *P. clarkii* tissues (Unpublished results). Similarity searches resulted in numerous hits which were manually inspected upon translation, using EMBOSS transeq (Rice et al., 2000), to identify those with features compatible with putative proline-rich AMPs (e.g. cationicity, proline and arginine residue distribution).

2.2. Phylogenetic analyses

The available draft genome of the marbled crayfish *Procambarus f. f. virginalis* (Gutekunst et al., 2018) was screened for the presence of astacidin using the four sequences identified in *P. clarkii* as queries. Significant hits (based on an e-value cutoff of $1\ E^{-5}$) were further inspected, fragmented contigs were re-assembled using the CLC Genomics Workbench v.11 (Qiagen, Hilden, Germany) and annotated upon alignment with genomic and cDNA sequences from congeneric species. Donor and acceptor splicing sites were refined using Genie (Reese et al., 1997).

Astacidin-like sequences were also searched for in other available transcriptomes from Astacidea, which were either downloaded from the NCBI TSA database (when available), or *de novo* assembled with the CLC genomics Workbench v.11, including those from: *Astacus astacus* (Theissinger et al., 2016), various *Cambarus* species (*C. cryptodytes*, *C. dubius*, *C. graysoni, C. hamulatus*, *C. nerterius*, *C. rusticiformis*, *C. setosus*) (unpublished), *Cherax cainii*, *C. destructor* (Ali et al., 2015), *C. quadricarinatus* (Tan et al., 2016), *Enoplometopus* cf. *daumi* MCZ IZ 74073 (unpublished), *Homarus americanus* (McGrath et al., 2016), *Nephrops norvegicus* (Rotllant et al., 2017), *Pacifastacus leniusculus* (unpublished), *Pontastacus leptodactylus* (Tom et al., 2014), various species of *Procambarus* (*P. fallax*, *P. horsti*, *P. lucifugus*, *P. pallidus*) (unpublished), *Orconectes (Faxonius) australis* and *O. (F.) incomptus* (unpublished). Positive hits were detected based on a minimum e-value threshold of $1\ E^{-3}$ and further refined based on detection by a custom HMM profile obtained from the multiple sequences alignment of the conserved signal peptide of all astacidins generated, using HMMER v.3.2.1 (Finn et al., 2011).

The phylogeny of astacidins was then inferred using MrBayes v.3.2.6 (Huelsenbeck and Ronquist, 2001), from the multiple sequence alignment of all available full-length astacidin sequences. The phylogenetic analysis was performed by running two independent Markov chain Monte Carlo (MCMC) analyses in parallel for 200,000 generations, until all estimated parameters of the model of molecular evolution (LG + G + I) reached an ESS value > 200.

2.3. Peptide synthesis

Three novel astacidin peptide sequences (PcAst-1a, 1b/c and −2) from *P. clarkii* were selected for chemical synthesis, based on suitable physico-chemical characteristics with respect to potential antimicrobial activity. The peptides were obtained from GenicBio (Shanghai, China) and SynPeptide (Shanghai, China), all at > 95% purity as confirmed by RP-HPLC and mass-spectrometry (PcAst-1a and -1b/c were synthesized as C-terminally amidated minus the terminal GK residues). Chromatographic separation was achieved on a reversed-phase column (C18, 5 μm, 4.6 × 250 mm) using a 1–70% acetonitrile/0.1% TFA gradient in 25 min at a 1 ml/min flow rate. Peptide stock concentrations were determined by dissolving accurately weighed aliquots of peptide in doubly distilled water, and further verified by using the extinction coefficients at 214 nm, calculated as described by Kuipers and Gruppen (2007).

2.4. Preparation of liposomes

Anionic and neutral LUVs (large unilamellar vesicles) were prepared by dissolving dry phosphatidylglycerol (PG) (Avanti Polar Lipids, Alabaster, Alabama, USA) or 1,2-dioleoyl-sn-glycero-3-phosphocholine (DOPC) (Avanti Polar Lipids), respectively, in chloroform/methanol (2:1) solution. The solution was evaporated in a small round-bottom flask under constant rotation, using a dry nitrogen stream and then vacuum-dried for 24 h. The liposome cake was resuspended in 1 ml of 10 mM sodium phosphate buffer (SPB) to a final concentration of 5 mM phospholipid and spun for 1 h at a temperature above the Tc (lipid critical temperature). The vesicle suspensions were then disrupted by several freeze–thaw cycles, from liquid N_2, prior to passage through successive polycarbonate filters with 1 μm, 0.4 μm and 0.1 μm pores, using a mini-extruder (Avanti Polar Lipids), and resuspended to a final phospholipid concentration of 0.4 mM. Considering liposome membrane surface area of a ~100 nm diameter liposome, and area of a phospholipid head group (~0.7–1 nm^2) (Tossi et al., 2000), the concentration of liposomes was estimated from the average number of phospholipids/liposomes to be about 5 nM.

2.5. Circular dichroism

CD spectra were obtained on a J-710 spectropolarimeter (Jasco, Tokyo, Japan), as the accumulation of three scans, and were measured

in a) SPB solution, b) 50% TFE in SPB, c) sodium dodecyl sulphate micelles (10 mM SDS in SPB), d) anionic LUVs (PG) in SPB or e) neutral LUVs (DOPC) in SPB.

2.6. Antimicrobial activity

The *in vitro* testing was carried by determining the minimal inhibitory concentration (MIC) against either reference (ATCC) laboratory strains (*Escherichia coli* ATCC 25922, *Acinetobacter baumannii* ATCC 19606 and *Staphylococcus aureus* ATCC 29213) or clinical isolates of these bacteria, some multi-drug resistant, as previously described in detail in Rončević et al. (2017). The MIC was assessed using the serial two-fold microdilution method according to the CLSI protocol (Clinical and Laboratory Standards Institute (CLSI), 2017). Bacteria were cultured in either full Mueller Hinton (MHB or 20% Mueller Hinton broth in SPB) to the mid exponential phase, and then added to serial dilutions of astacidin peptides to a final load of 5×10^5 CFU/ml in 100 µl per well, and incubated at 37 °C for 18 h. The MIC was visually determined as the lowest concentration of the peptide showing no detectable bacterial growth, and accepted if it was the consensus value of an experiment performed in triplicate.

For determination of minimal bactericidal concentration (MBC), 4 µL of bacterial suspensions were taken from the wells corresponding to MIC, 2 × MIC, and 4 × MIC and then plated on MH agar plates. Plates were incubated for 18 h at 37 °C to allow the viable colony counts and the MBC determined as the peptide concentration causing no visible growth.

2.7. Cytotoxicity assay

The cytotoxic effect of astacidin peptides was determined on both lymphoid and epithelial cell line models. For *in vitro* maintenance, the human MEC-1 lymphoid tumour cell line (Stacchini et al., 1999) was cultured in RPMI 1640 medium supplemented with 2 mM L-glutamine, 100 U/mL penicillin, 100 µg/mL streptomycin, and 10% fetal bovine serum (FBS) (complete medium) and sub-cultured two-three times a week for not more than 20 passages; the epithelial cell lines (human bladder cancer cell lines T24 and TCCSUP) purchased from ATCC (LGC Standards, Teddington, Middlesex, UK), were sub-cultured in a Dulbecco's modified Eagle's medium (DMEM Euroclone, Milano, Italy) containing 4.5 g/L glucose, 10% fetal bovine serum (FBS) and antibiotics (100 U/mL penicillin, 100 µg/mL streptomycin).

Cytotoxicity assays were carried out by seeding cells into 96-well culture plates; MEC-1 were diluted to 10^6 cells/ml and treated with astacidin peptides for 24 h, after which 20 µL of MTT dye (5 mg/mL) was added to each well and incubated for 4 h at 37 °C. Formazan crystals were solubilized with acidic isopropanol (0.04 N HCl in absolute isopropanol) and the absorbance measured at 540 nm and 630 nm with microplate reader (Tecan Sunrise, Männedorf, Switzerland). T24 and TCCSUP epithelial cell lines were sown at a density of 3×10^5 cells/ml and treated with astacidin peptides for 4, 24, 48 and 72 h, after which cells were incubated with MTT dye (0.5 g/L) at 37 °C for 2 h. Formazan crystals were solubilized with 10% dimethylsulphoxide (DMSO) and formazan formation was measured at 570 nm with ELx808 Ultra Microplate Reader (BioTek, Inc., Winooski, Vermont, USA).

All measurements were done at least in triplicate and the data were calculated in relation to the untreated control (100%).

2.8. Animal maintenance

Twenty adult *P. clarkii* females, at intermolt stage (body weight 37 ± 8 g), were collected from an artificial river inside the "Bonifica del Brancolo" (45°46′ N, 13°30′ E, GO, Italy) and kept in two separate 120 L tanks provided with closed circuit filtered and thoroughly aerated tap water at ~18 °C. They were fed fish pellets (Sera granular, Heisenberg, Germany) three times a week, for a week, before the start of the experiment.

The experiments on these animals complied with the current laws of Italy, the country where these were performed. No specific permits were required for studies that did not involve endangered or protected species. Individuals were maintained in appropriate laboratory conditions to guarantee their welfare and responsiveness. After the experiments were completed, the crayfish were sacrificed by hypothermia.

2.9. LPS-challenge in P. clarkii

Two groups of three crayfish each were injected with 0.025 µg/g body weight of lipopolysaccharide from *E. coli* O111:B4 (Sigma) solubilized in PBS 1X in the abdominal cavity and sacrificed at 2 and 4 h post-injection. In parallel, two control groups, consisting of 3 crayfish each, for the two experimental points considered, were injected with crustacean saline solution (NaCl 14.5 g, $CaCl_2$ 0.72 g, $MgSO_4$ 3.18 g, KCl 0.35 g, HEPES 5 mM, $NaHCO_3$ 0.5 g at pH 7.4 in a final volume of 1.2 L), and also sacrificed at 2 and 4 h post-injection.

Haemolymph was withdrawn with a 10 ml needle-less syringe and haemocytes were pelleted through centrifugation at 4°C, 2000 xg for 1 min.

2.10. Gene expression analysis

The basal expression levels of astacidins in naïve animals were evaluated through the analysis of RNA-seq data from 12 tissues (brain, eyestalk, green glands, ventral ganglia, heart, hepatopancreas, gills, haemocytes, muscle, Y-organ and epidermis, ovary and testis) Illumina sequenced (depth 2x100 bp), derived from a transcriptome study (Unpublished results).

The CLC Genomics Workbench v.12 (Qiagen, Hilden, Germany) was used to map the reads from each tissue to the assembly, using the RNA-seq analysis tool with the following parameter settings: mismatch cost 2, gap insertion and deletion costs 3, end gaps 0, length fraction 0.95, similarity fraction 0.98.

The total RNA from LPS-challenged crayfish was extracted from haemocytes by following the TRI Reagent® (Sigma-Aldrich) manufacturer's protocol. The concentration and quality of extracted RNAs were checked using an Agilent 2100 Bioanalyzer and the RNA 6000 Nano kit (Agilent Technologies). cDNAs were produced using the GoTaq 2 Step RT qPCR kit (Promega), starting from 1 µg of total RNA and following the manufacturer's instructions. A dilution of 1/5th of the initial cDNA was used for quantitative-Real Time PCR (qRT-PCR) validations.

Specific primers were designed through Primer3Web version 4.0.0 (Untergrasser et al., 2012) and Oligo Calculator version 3.26 (Kibbe, 2007) to predict possible secondary structures and hairpin formations, as reported in Table 1.

The qRT-PCR reactions were performed in triplicate on experimental samples by using the PerfeCTa SYBR® Green supermix (Quanta bio), and following the thermal cycle: initial denaturation 95 °C for 2'; 35 cycles composed of two-steps reaction 95 °C for 1″, annealing and elongation 60 °C for 30"; followed by a melting curve from 65 °C to 95° with a temperature increment of 0.5 °C every 5". Each PCR reaction was performed in a final volume of 15 µl, with a final concentration of 1 X supermix, 0.3 µM of each primer and 1 µL of cDNA.

The Elongation Factor 1-alpha (EF1α), previously validated as stable reference gene for qPCR analyses in *P. clarkii* (Manfrin et al., 2015), was used for internal normalization across samples. The CFX Maestro software (Bio-Rad) was used to calculate the relative expression of different astacidins among the experimental samples, following the ΔΔCt method. Differentially expressed genes were identified using the Shapiro-Wilk test, based on a p-value threshold of 0.05.

3. Results and discussion

3.1. Astacidin identification

The putative AMP cDNA sequences identified in *P. clarkii* thanks to their similarity with the signal peptide of the previously reported *P.*

Table 1
Primers used for qRT PCR validation. EF1α: Elongation factor 1 alpha served as reference gene. bp: base pairs.

Primer ID	Forward	Reverse	Amplicon size (bp)
EF1α	AGATCTGAAACGTGGTTTTGTT	TCAATCTTTTCCAGAAGTTCGT	186
Pc-Ast-1 a	TCCCGCCTACCGTCCT	CAAGAGGGAAGGGAAGCC	115
Pc-Ast-1 b/c	ACTTCGCCGTCCTGGCTA	TGTGGCTGGTGATGGTAGAG	103
Pc-Ast-2	TGACTGGAGGATCACAACTCT	GTAAGGGCGGGGATAAAAAG	122
Pc-Ast-3	TGACTGGAGGATCACAACTCT	CCTCAGTGGACGGTCAGG	134

leniusculus astacidin (Jiravanichpaisal et al., 2007) were translated and analysed, looking for typical features of PR-AMPs (cationic charge, a pattern of alternating proline and arginine residues). The query sequence had been originally assigned the suffix "-2" by Jiravanichpaisal et al. due to the previous discovery of the unrelated hemocyanin-derived AMP Astacidin 1 from the same species (Lee et al., 2003). However, to avoid nomenclature confusion in future assignments and to maintain consistency with phylogenetic evidence (see section 3.2), we will hereafter refer to this peptide as *Ple*Astacidin-1 (see Table 2), and consider its orthologous AMPs as members to the astacidin-1 clade.

The first AMP identified in *P. clarkii* was named PcAst-1a, and its 43 aa long precursor displays a well supported signal peptide, which would result, upon proteolytic cleavage, in a mature PR-AMP of 20 aa, with a C-terminal amidation signal. Another slightly longer mature peptide (25 residues) was assigned the name PcAst-1b, with an additional variant ($His_5 \rightarrow Tyr_5$ within the signal peptide region) named PcAst-1c.

A fourth sequence, named PcAst-2, perfectly matched a transcript upregulated in the haemocytes of white spot syndrome virus-infected *P. clarkii* (Shi et al., 2010). This 31 aa long PR-AMP, produced by the proteolytic cleavage of a 53aa long precursor, was found to be significantly different and longer than the three Astacidin-1 isoforms, and lacked the GK amidation signal (see Table 2). An additional 50 aa long precursor sequence, named PcAst-3, shared close similarity with PcAst-2 in its N-terminal region, but had a shorter mature peptide (28 aa), which contained the GK amidation signal at the end of an anionic Tyr-rich C-terminal section (see Fig. 1a).

All *P. clarkii* astacidins, as well as the orthologous sequences from other crustaceans (see Table 2 and section 3.2), have a content and distribution of proline and arginine residues consistent with their classification within the class of PR-AMPs (Scocchi et al., 2011). Besides crustaceans (e.g. mud crab PR-AMPs, crab arasins and shrimp penaeidins), this type of AMPs is also found in insects (e.g. apidaecins, pyrrhocoricins, drosocins, oncocyns) (Bulet et al., 1999; Otvos, 2000) and artiodactyl mammalian species (e.g. bactenecins) (Scocchi et al., 2011). Among marine invertebrates, PR-AMPs have been also occasionally described in molluscs, such as in the case of mussel myticalins (Leoni et al., 2017) and oyster Cg-Prp (Gueguen et al., 2009).

However, no significant sequence similarity was observed between astacidins and other PR-AMP families, with the possible exception of a central motif in the PcAst-2 sequence (RPPYLPxPxPxPRPxPxF) (see Fig. 1b), which is present in cetartiodactyl cathelicidin PR-AMPs as well as in insect oncocin (Knappe et al., 2010; Mardirossian et al., 2018; Scocchi et al., 2011). This may represent an interesting case of convergent evolution pointing to a conserved sequence motif that may be functionally relevant for PR-AMPs, regardless of their origin. In this respect, it should be pointed out that some PR-AMPs, including those listed in Fig. 1.b, have a mode-of-action which involves their translocation into susceptible bacteria via a membrane transporter, and the subsequent inactivation of bacterial ribosome subunits (Graf et al., 2017).

3.2. Gene architecture and taxonomical distribution of astacidins

We investigated the gene structure of astacidins in *P. virginalis*, the only species of this genus with a genome currently available. In spite of its highly fragmented nature (nearly 2 million scaffolds with a N50 close to 1 kb), we could retrieve one full-length astacidin gene (orthologous to PcAst-2, i.e. sharing 98% sequence identity at the nucleotide level within the CDS) and an additional partial hit for a gene orthologous to PcAst-3 (i.e. sharing 95% sequence identity at the nucleotide level). No sequences orthologous to PcAst-1a or -1b/c could be detected.

*Pvi*Astacidin-2 displays a genomic architecture comprising two exons and a phase 2 intron splitting the open reading frame close to its 3'end (Fig. 2). Although the 5′ and 3′ boundaries of the gene could not be defined with certainty, due to the absence of mRNA data for this species, the alignment with the *P. clarkii* cDNA permitted to define a first exon comprising at least 367 nucleotides, a 685 nucleotides-long intron and a second exon comprising at least 866 nucleotides, of which the 3'end was well supported by the presence of a potential AATAAA mRNA polyadenylation site. The *Pvi*Astacidin-3 ortholog is only a partial sequence that however includes the entire sequence of exon 1, which contains the complete ORF, implying that, in this case, exon 2 only includes the 3′UTR sequence.

Numerous astacidin orthologous sequences were identified in the transcriptomes of several crayfish species of the superfamily Astacoidea (see Table 2), in spite of the absence of RNA-seq data specifically obtained from circulating haemocytes, the main tissue of production of these AMPs (see section 3.5). Phylogenetic inference suggests that all astacidins derive from two ancestral lineages, of which members can now be found in most (if not all) crayfish species (see Fig. 3). These two lineages correspond to PcAst-1a and PcAst-2/3 orthologs, respectively. In particular, sequences orthologous to PcAst-2 and -3 could be found, with minor variations, in multiple *Procambarus* and *Cambarus* species, as well as in *A. astacus*, *P. leptodactylus* and *P. leniusculus* (Fig. 3). Members of the Astacidin-1 lineage were detected in different *Procambarus*, *Cambarus* and *Orconectes* (*Faxonius*) species, as well as in *P. leniusculus*. *P. clarkii* was the only species where a gene duplication event, originating PcAst-1a and -1b/c, was apparent.

Although transcriptomic screening suggests that no astacidin-like sequences are present in two of the four Astacidea superfamilies (Enoplometopoidea and Nephropoidea), astacidin-like sequences were found in *Cherax* spp., indicating a taxonomical distribution covering both Astacoidea and Parastacoidea. While one of the sequences identified in *C. quadricarnatus* (*Cqu*Astacidin-X1) belonged to the main clade including all Astacoidea astacidins (and may be more closely related to the Astacidin-1 group, see Table 2), two orthologous sequences from *C. cainii* and *C. quadricarnatus* (*Cqu*Astacidin-X2 and *Cqu*Astacidin-X2) clustered in a divergent, basal lineage (Fig. 3).

Overall, in spite of the remarkable sequence divergence in the antimicrobial peptide region, all astacidins were defined as being characterized by a highly conserved, 22 aa long signal peptide, which might be effectively used for classification purposes, and for which the 50% majority rule consensus was MRLLYLLXLVLVALMAAVPSQA. With respect to the AMP domain, astacidin-2 orthologs and the two divergent *Cherax* spp. sequences both lacked the characteristic GK C-terminal amidation motif present in all other astacidins.

No orthologous sequences were detected in the transcriptomes of other, non-Astacidean decapods, indicating that astacidins represent a taxonomically restricted gene family (Khalturin et al., 2009) or that any orthologous sequences in other crustaceans are too divergent from those of Astacidea to enable detection by homology-based methods.

Table 2
Sequence and properties of astacidin peptides identified in different Astacidae species.

Peptide	Species	Family	Sequence[1,2]
Astacidin 1			----:----|----:----|----:----|
PcAst-1a (*)	*Procambarus clarkii*	Cambaridae	SNGYRP-------AYRPAYRPSYRP*GK*
*Ple*Astacidin-1§	*Pacifastacus leniusculus*	Astacidae	SLGYRP-----RPNYRP--RPIYRPGK
PcAst-1 b/c (*)	*P. clarkii*	Cambaridae	SNVYRPPPY--RPVYRPLRRPGYRP*GK*
*Plu*Astacidin-1	*P. lucifugus*	"	SHGYRPPYLP-----RPRPRPIYRP*GK*
*Cgr*Astacidin-1	*Cambarus graysoni*	"	SSGHRPIYRPPRPIYRPLPRPIYRP*GK*
*Chu*Astacidin-1	*C. humulatus*	"	SNGHRPIYRPPRPIYRPLPRPVYRP*GK*
*Cdu*Astacidin-1	*C. dubius*	"	SNGHRPIYRPPRPIYRPQPRPIYRP*GK*
*Cne*Astacidin-1	*C. nerterius*	"	SNGHRPIYRPPRPIYRPQPRPIYRP*GK*
*Cru*Astacidin1	*C. rusticiformis*	"	SNGHRPIYRPPRPIYRPLPRPIYRP*GK*
*Oau*Astacidin-1	*Orconectes (Faxonius) australis*	"	SNGHRPIYRPPRPIYRPLPRPVYRP*GK*
OinAstacidin-1	*O. (F.) incomptus*	"	SNGHRPIYRPPRPIYRPLPRPVYRP*GK*
*Cqu*Astacidin-X1	*Cherax quadraticus*	Parastacidae	GRHQRPYLPRPRYRP*GK*
Astacidin 2			----:----|----:----|----:----|
PcAst-2 (*)	*P. clarkii*	Cambaridae	FYPRPYRPPYLPDPRPFPRPLPAFGHEFRRH
*Ppa*Astacidin-2	*P. pallidus*	"	FYPRPYRPPYLPDPRPFPRPLPAFGNEFRRH
*Plu*Astacidin-2	*P. lucifugus*	"	FYPRPYRPPYLPDPRPFPRPLPAFGNEFRRH
*Pvi*Astacidin-2	*P. virginalis*	"	FYPRPYRPPYLPDPRPFPRPLPAFGNEFRRH
*Pfa*Astacidin-2	*P. fallax*	"	FYPRPYRPPYLPDPRPFPRPLPAFGNEFRRH
*Pho*Astacidin-2	*P. horsti*	"	FYPRPYRPPYLPDPRPFPRPLPAFGNEFRRH
*Cgr*Astacidin-2	*C. graysoni*	"	FYPRPYRPPYLPDPRPFPRPLPAFGDGYRPR
*Cne*Astacidin-2	*C. nerterius*	"	FYPRPYRPPYLPDPRPFPRPLPAFGDGYRPR
*Cru*Astacidin-2	*C. rusticiformis*	"	FYPRPYRPPYLPDPRPFPRPLPAFGDGYRPR
*Cte*Astacidin-2	*C.tenebrosus*	"	FYPRPYRPPYLPDPRPFPRPLPAFGDGYRPR
*Aas*Astacidin-2	*A. astacus*	Astacidae	FYPQPFRPPYVPDPRPFPRPFPAYDAI
*Ple*Astacidin-2§	*P. leniusculus*	"	FYPRPYRPPYLPDPRPFPRPLPAYDAI
Astacidin 3			----:----|----:----|----:----|
PcAst-3	*P. clarkii*	Cambaridae	FIPRPDRPLRPYPRPFVDYGDYGIYG*GK*
*Pvi*Astacidin-3	*P. virginalis*	"	YIPRPDRLLRTYPRPFVDYGDYGIYG*GK*
*Cte*Astacidin-3	*C. tenebrosus*	"	YIPRPYRPLR-YPRPFVDYGDYGIYG*GK*
*Aas*Astacidin-3	*A. astacus*	Astacidae	FIPRPYRPPRPYPRPFVDYGDYGIYG*GK*
*Ple*Astacidin-3	*P. leniusculus*	"	FIPNPYRQPRPYPKPFVDYGDYGIYG*GK*
Others			----:----|----:----|----:----|
*Cqu*Astacidin-X2	*C. quadraticus*	Parastacidae	LRFDPYYPVWPEYRPHYFPPPVYYK
*Cca*Astacidin-X2	*C. cainii*	"	LRFDPYYPSWPEYRPHYFPPPVYYK

1) Residues that are conserved in ≥50% of peptides in any astacidin peptide family are shaded.
2) Astacidin peptides with GK (italic, underlined) as C-terminal residues are likely amidated at the third last residue.
(*) These sequences were selected for peptide synthesis and functional characterization.
(§) As explained in the text, *Ple*Astacidin-1 had been previously designed as astacidin-2 by Jiravanichpaisal et al. (2007); to avoid nomenclature confusion and maintain consistency with phylogenetic evidence (see section 3.2), we renamed this sequence *Ple*Astacidin-1 and re-assigned the name *Ple*Astacidin-2 to a newly identified AMPs supported by transcriptomic evidence.

3.3. Peptide structure

The CD spectra for PcAst-1a, -1b/c and −2 in aqueous phosphate buffer were compatible with an extended conformation, which was not surprising given the high content of proline (incompatible with a helical conformation) and relatively short size of the peptides (unlikely to lead to β-hairpin formation) (Fig. 4). In the presence of SDS micelles, all spectra became more positive in the region about 230 nm, suggesting a possible contribution from a polyproline type-II conformation under these conditions. There is little change in spectra in the presence of LUVs formed by DOPC, suggesting that the peptides do not interact with neutral biological membranes. There was instead a significant change in the spectra of all the peptides in the presence of anionic LUVs formed by PG. Furthermore, these spectra resembled those in the presence of the organic solvent TFE. This suggests that the peptides interact with the surface of anionic biological membranes, likely via electrostatic interactions, and that they then are susceptible to the anisotropic environment at the membrane surface. In any case, results would point to a preferred interaction with bacterial rather than animal cells, which might result in a more significant effect on the former.

AMP name	Peptide sequence
1.a	
PcAst-1a	MRLLHLLLSVALVALMAAVPSQA-**SNGYRPAYRPAYRPSYRPGK**
PcAst-1b	MRLLHLLLSVALVALMAAVPSQA-**SNVYRPPPYRPVYRPLRRPGYRPGK**
PcAst-1c	MRLLYLLLSVALVALMAAVPSQA-**SNVYRPPPYRPVYRPLRRPGYRPGK**
PcAst-2	MRLLHLQALVLMVLMAAVPSQA-**FYPRPYRPPYLPDPRPFPRPLPAFGHEFRRH**
PcAst-3	MRLLHLLALLLVALMTAVPSQA-**FIPRPDRPLRPYPRPFVDYGDYGIYGGK**
1.b	
PcAst-2	FYPRPYRPPYLPDPRPFPRPLPAFGHEFRRH
Bac7 (bovine)	RRIRPRPPRLPRPRPRPLPFPRPGPRPIPRPL
Tur1 (dolphin)	RRIRFRPPYLPRPGRRPRFPPPFPIPRIPRIP
PR-29 (Pig)	RRRPRPPYLPRPRPPFFPPRLPPRIPPGFPPRFPPRFP
Oncocyn1 (bug)	VDKPPYLPRPPPPRRIYNNR

Fig. 1. a. Alignment of Pc astacidin precursors. **1.b** Alignment of PcAst-2 with PR-AMPs from cetartiodactyl cathelicidins and insect oncocin. Residues conserved with respect to PcAst-2 are shaded.

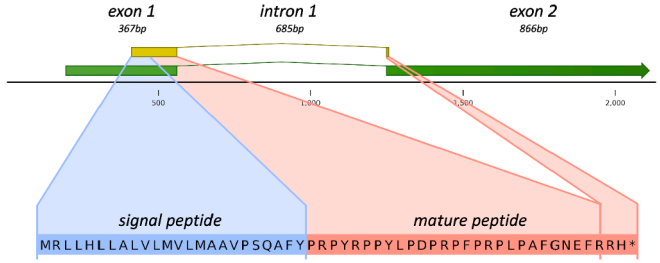

Fig. 2. Genomic architecture of the *Pvi*Astacidin-2 gene. The translated sequence of the peptide precursor is displayed below, with the signal peptide and mature peptide regions coloured in blue and red, respectively. The ORF is split, within the mature peptide region, by a phase 2 intron. The coding sequence is displayed in yellow and the putative mRNA sequence in green.

3.4. Biological activity

PcAst-1a, -1b/c and −2 have been tested for antimicrobial and cytotoxic properties as assessed on human transformed cells. Activity against bacterial cells was generally low (> 32 μM) in full MH medium, while in 20% MH broth it ranged from poor (≥32 μM for PcAst-1a), to selectively active (e.g. PcAst-2 against *A. baumannii*) to potent and broad-spectrum against both Gram-negative and Gram-positive strains (PcAst-1b/c) (see Table 3). In the latter case, it is worth noting that activity extends to antibiotic-resistant clinical isolates of both *E. coli* and *A. baumannii,* (MBC = 2–4 μM). Interestingly, PcAst-1a did not show an increase in antimicrobial activity even in the reduced MH medium, in contrast with previous findings (Shi et al., 2014), suggesting it may become active only in nutrient and salt deprived media such as those used in that study [c.f. 1% tryptone, 0.5% NaCl (w/v)].

The potency of AMPs in general correlates with cationicity, and the activity of PR-AMPs is normally directed towards susceptible Gram-negative species, as this type of peptide is known to internalize via a specific translocation system and inactivate internal targets (ribosomes and the chaperone dnaK) (Graf et al., 2017; Mardirossian et al., 2014; Paulsen et al., 2016; Runti et al., 2013). It is therefore not surprising that the astacidins are more aggressive against the Gram-negative bacteria. It will be interesting to determine if the potency against Gram-negative species is due to intracellular translocation through the known transporter SbmA (Runti et al., 2013), which is present in both *E. coli* and *A. baumannii*. Concerning the cationicity, the higher charge of PcAst-1b/c (+7) may explain its greater potency than the longer but less charged PcAst-2 (+4/5 depending on the state of the His residue), which, unusually for PR-AMPs, has two anionic residues. It is interesting to note that an up-regulation of the PcAst-2 gene has been previously reported in response to viral, rather than bacterial, infection (Shi et al., 2010).

Activity was also tested against the MEC-1 lymphoid and two human bladder epithelial cancer cell lines, TCCSUP and T24, respectively. None of the *P. clarkii* astacidins showed observable cytotoxic effects on the MEC-1 lymphatic leukaemia cell line (up to highest concentrations tested, 100 μM) as determined by the MTT assay. No significant activity was observed against the T24 cells for all tested concentrations and exposure times, with IC_{50} values being well above 100 μM for all three peptides. A weak, dose and time dependent activity was instead detected against the TCCSUP cell line, with an estimated IC_{50} value of ~70 μM for PcAst-1a and −2, and ~100 μM for PcAst-1b/c, after 72 h. These results suggest that the peptides are not significantly cytotoxic towards epithelial animal cells, at antimicrobial

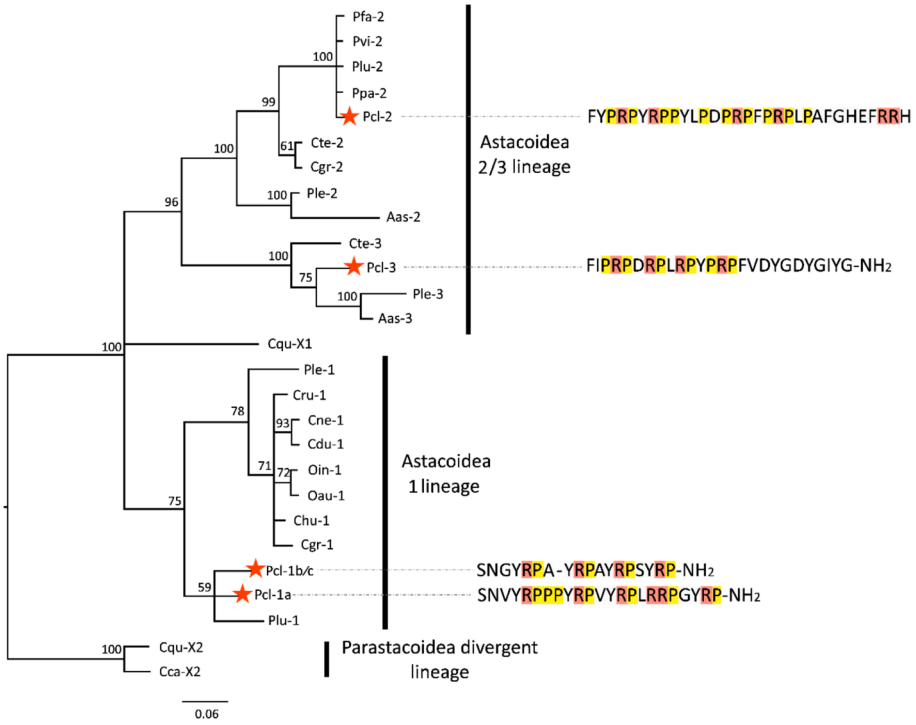

Fig. 3. Bayesian phylogeny of astacidins, based on the multiple sequence alignment of full-length peptide precursors. Posterior probability values are shown for each node of the tree. The four sequences of *P. clarkii* are marked with a red star and the corresponding predicted mature peptide is indicated on the side of the tree. Arginine and proline residues are indicated in red and yellow, respectively. The tree was arbitrarily rooted using the Parastacoidea divergent lineage as an outgroup. Each sequence is indicated with a three letters code derived from the first letter of the genus and first two letters of the species names, respectively. See the main text for details.

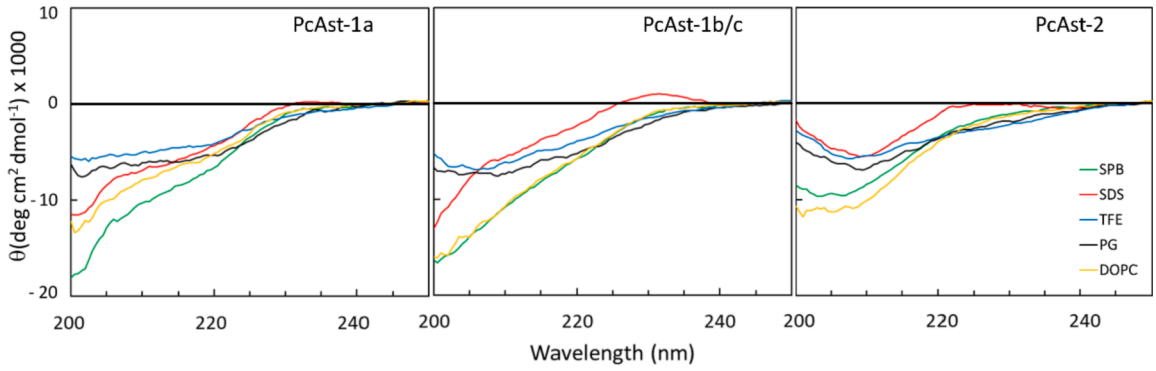

Fig. 4. CD spectra for *P. clarkii* astacidins under different conditions. Spectra are the accumulation of three scans carried out with 20 μM peptide in aqueous buffer, in the presence of TFE and SDS micelles or anionic (phosphatidylglycerol, PG) or neutral (dioctanoyl phosphatidylcholine, DOPC) LUVs, representing model biological membranes.

Table 3
Antimicrobial activity of astacidin peptides in 20% MH expressed as Minimum Inhibitory Concentration (MIC) and Minimum Bactericidal Concentration (MBC) both expressed in μM).

Bacterial strains	PcAst-1a		PcAst-1b/c		PcAst-2	
	MIC	MBC	MIC	MBC	MIC	MBC
S. aureus ATCC 29213	32	> 32	2	4	32	32
S. aureus c.i.	> 32	/	32	> 32	> 32	/
E. coli ATCC 25922	32	> 32	1	1	32	> 32
E. coli c.i.	> 32	/	2	2	> 32	/
A. baumannii ATCC 19606	> 32	/	2	4	8	8
A. baumannii c.i.	> 32	/	2	4	8	8

Table 4
Astacidins and EF1α gene expression in 12 different tissues. Expression levels are shown as TPMs (Transcripts Per Million) values and quantified using a coloured scale. Black > 2000, dark grey (2000-500), mid grey (499-100), light grey (99-10), white < 10 TPMs.

Astacidin	Brain	Eyestalk	Haemocytes	Green glands	Ventral ganglia	Y organ	Hepatopancreas	Heart	Testis	Ovary	Gills	Muscle
PcAst-1a	494	128	7729	109	369	187	10	169	19	48	1420	21
PcAst-1b/c	612	71	4458	45	183	103	4	74	14	24	1048	12
PcAst-2	13	7	309	5	15	6	0	5	2	3	24	2
PcAst-3	11	5	183	3	17	7	1	7	3	1	22	1
Ef1a	1340	955	1614	1600	1594	1076	740	1110	807	1423	1185	649

concentrations, although some specific types of cells may be more susceptible than others. This is in line with the prediction made based on CD spectra (see above).

3.5. Astacidins expression in P. clarkii

Following the transcriptomic characterisation of PcAst-1a, PcAst-1b, PcAst-1c, PcAst-2 and PcAst-3, their expression has been quantified using available RNAseq data collected from 12 different tissues of naïve (unexposed to bacteria or PAMPs) *P. clarkii*. Table 4 shows the Transcripts per Million (TPM) obtained from the RNA-seq analysis on these 12 different tissues. PcAst-1b and -1c have been clustered together since they differ only in a single amino acid within the signal peptide region.

Despite significant differences among the five isoforms, haemocytes clearly represent the specific compartment for expression of all five astacidins under naïve conditions. PcAst-1a, and -1b/c are the most

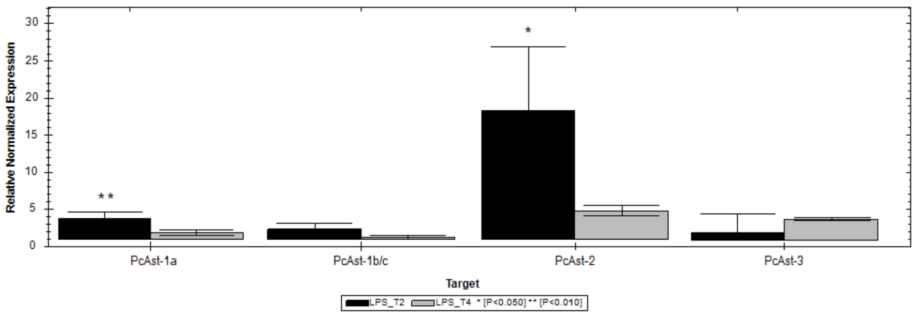

Fig. 5. Relative expression of *P. clarkii* astacidins in haemocytes following LPS-challenge at 2 and 4 h post injection (LPS_T2 and LPS_T4. respectively). The ΔΔCt method was applied by using control groups and EF1-α as calibrator samples. Statistically significant p-values are indicated by asterisks.

expressed in haemocytes (~7700-4400 TPMs), and were also found in gills (~1400-1000 TPMs, about 5-fold less expressed than haemocytes). PcAst-2 was also expressed at a significant level in haemocytes (~300 TPMs, about 24-fold less than PcAts-1a), but its expression fell in barely detectable in all the other tissues. PcAst-3 reached a level of ~180 TPMs in haemocytes, being the least expressed astacidin isoform (42-fold less than PcAst-1a). In general, astacidins were poorly expressed in all the other tissues, including hepatopancreas, which suggests that astacidins are strictly involved in haemocyte-mediated immunity.

Although the presence of PcAst1a in the gills of naïve animals supports the findings of Shi and colleagues that PcAst expression could be induced in the gills as well (Shi et al., 2014), this observation could also be explained by the presence of the haemolymph in the gills, since this tissue is in direct contact with the open circulatory system (Burggren et al., 1974). The pattern of inducibility of the newly characterized PcAsts was experimentally investigated by the withdrawal of haemolymph from healthy *P. clarkii* female individuals in intermolt, 2 and 4 h post- LPS-injection.

The relative expression of astacidins was then estimated using qRT-PCR, using the elongation factor 1 alpha (EF1α) as a reference gene. The ΔΔCt method was applied to detect statistically significant differences with a non-challenged (buffer injected) control group, at two selected time points (Fig. 5). The results indicated a significant up-regulation of PcAst-1a and PcAst-2 at 2 h post injection (p-value < 0.0095 and < 0.0201, respectively), whereas none of the four astacidins tested were differentially regulated 4 h after the injection. The early inducibility of PcAst-1a and PcAst-2 suggests their possible involvement in an early-defence against Gram-negative bacteria infection. On the other hand, the lack of modulation of PcAst-1b, -1c and PcAst3 in response to LPS-challenge suggests that the expression of these AMPs may be induced by other PAMPs, not necessarily associated with the Gram-negative bacterial cell wall.

4. Conclusions

Three different types of astacidin proline rich AMPs (PR-AMPs) were identified in several crayfish species from the superfamily Astacoidea. Phylogenetic inference, together with the screening of available sequencing data, allowed the identification of orthologous sequences also in members of the Parastacoidea superfamily. RNAseq analyses pointed out that all members of the PcAst-1 class are highly expressed in haemocytes of naïve crayfish, and to a lesser extent also in gills, showing a high basal expression level and a strong tissue-specificity. The inducibility of PcAst-1a and PcAst-2 on challenge with LPS, suggests that PcAsts are involved in the immune response, while the triggering elements remain to be identified for PcAst-1b/c and −3. Primary structural features (high number of Pro residues) and circular dichroism studies suggest that these peptides have a simple linear structure and might interact selectively with the surface of anionic biological membranes. It still remains to be determined whether the activity of astacidins on Gram-negative bacteria depends on their internalization and subsequent inactivation of ribosomes, as reported for other mammalian and insect PR-AMPs that share a conserved sequence motif.

Data deposition

PcAst nucleotide sequences have been deposited at GenBank under the following accession numbers: PcAst-1a_astacidin MN848347; PcAst-1b_astacidin MN848348; PcAst-1c_astacidin MN848349; PcAst-2_astacidin MN848350; PcAst-3_astacidin MN848351.

Declaration of competing interest

All authors listed on the paper declare to have no conflict of interest of any nature both financial, personal and related to other people or organizations.

Acknowledgments

The authors would like to thank Dr. Paolo Macor from Department of Life Sciences, University of Trieste for kindly supplying human MEC-1 cell line and the Laboratory for Clinical Microbiology at the University Hospital Centre Split, Croatia for providing clinical bacterial isolates used in the study.

References

Ali, M.Y., Pavasovic, A., Amin, S., Mather, P.B., Prentis, P.J., 2015. Comparative analysis of gill transcriptomes of two freshwater crayfish, *Cherax cainii* and *C. destructor*. Mar. Genomics 22, 11–13.

Boguski, M.S., Lowe, T.M.J., Tolstoshev, C.M., 1993. dbEST — database for "expressed sequence tags". Nat. Genet. 4, 332–333.

Bulet, P., Hetru, C., Dimarcq, J.L., Hoffmann, D., 1999. Antimicrobial peptides in insects; structure and function. Dev. Comp. Immunol. 23, 329–344.

Burggren, W.W., McMahon, B.R., Costerton, J.W., 1974. Branchial water- and blood-flow patterns and the structure of the gill of the crayfish *Procambarus clarkii*. Can. J. Zool. 52, 1511–1518.

CLSI, 2017. In: Performance Standards for Antimicrobial Susceptibility Testing in: Clinical and Laboratory Standards Institute, C., 27th ed. Clinical and Laboratory Standards Institute, (CLSI), Wayne, PA.

Cuthbertson, B.J., Deterding, L.J., Williams, J.G., Tomer, K.B., Etienne, K., Blackshear, P.J., Büllesbach, E.E., Gross, P.S., 2008. Diversity in penaeidin antimicrobial peptide form and function. Dev. Comp. Immunol. 32, 167–181.

Dai, L.S., Abbas, M.N., Kausar, S., Zhou, Y., 2017. Transcriptome analysis of hepatopancreas of *Procambarus clarkii* challenged with polyriboinosinic polyribocytidylic acid (poly I:C). Fish Shellfish Immunol. 71, 144–150.

Destoumieux, D., Bulet, P., Loew, D., Van Dorsselaeri, A., Rodriguez, J., Bachère, E., 1997. Penaeidins, a new family of antimicrobial peptides isolated from the shrimp *Penaeus vannamei* (Decapoda). J. Biol. Chem. 272, 28398–28406.

Du, Z., Jin, Y., Ren, D., 2016. In-depth comparative transcriptome analysis of intestines of red swamp crayfish, *Procambarus clarkii*, infected with WSSV. Sci. Rep. 6.

Finn, R.D., Clements, J., Eddy, S.R., 2011. HMMER web server: interactive sequence similarity searching. Nucleic Acids Res. 39, 29–37.

Ganz, T., Lehrer, R.I., 1994. Defensins. Curr. Opin. Immunol. 6, 584–589.

Gong, L., Shu, X., Zhang, C., Xiong, B., Yang, L., Gu, Q., Chen, J., 2012. Status and prospect of crop rotation of *Procambarus clarkii* and mid-season rice in China. Advances in Intelligent and Soft Computing 134, 283–291.

Graf, M., Mardirossian, M., Nguyen, F., Seefeldt, A.C., Guichard, G., Scocchi, M., Innis, C.A., Wilson, D.N., 2017. Proline-rich antimicrobial peptides targeting protein synthesis. Nat. Prod. Rep. 34, 702–711.

Gueguen, Y., Bernard, R., Julie, F., Paulina, S., Delphine, D., Franck, V., Philippe, B., Evelyne, B., 2009. Oyster hemocytes express a proline-rich peptide displaying synergistic antimicrobial activity with a defensin. Mol. Immunol. 46, 516–522.

Gutekunst, J., Andriantsoa, R., Falckenhayn, C., Hanna, K., Stein, W., Rasamy, J., Lyko, F., 2018. Clonal genome evolution and rapid invasive spread of the marbled crayfish. Nature Ecology and Evolution 2, 567–573.

Hancock, R.E., Diamond, G., 2000. The role of cationic antimicrobial peptides in innate host defences. Trends Microbiol. 8, 402–410.

Hoffmann, J.A., Kafatos, F.C., Janeway, C.A., Ezekowitz, R.A., 1999. Phylogenetic perspectives in innate immunity. Science 284, 1313–1318.

Huelsenbeck, J.P., Ronquist, F., 2001. MRBAYES: Bayesian inference of phylogenetic trees. Bioinforma. Oxf. Engl. 17, 754–755.

Imjongjirak, C., Amphaiphan, P., Charoensapsri, W., Amparyup, P., 2017. Characterization and antimicrobial evaluation of SpPR-AMP1, a proline-rich antimicrobial peptide from the mud crab *Scylla paramamosain*. Dev. Comp. Immunol. 74, 209–216.

Jin, S., Jacquin, L., Huang, F., Xiong, M., Li, R., Lek, S., Li, W., Liu, J., Zhang, T., 2019. Optimizing Reproductive Performance and Embryonic Development of Red Swamp Crayfish *Procambarus clarkii* by Manipulating Water Temperature Aquaculture, vol. 510. pp. 32–42.

Jiravanichpaisal, P., Lee, S.Y., Kim, Y.A., Andren, T., Söderhäll, I., 2007. Antibacterial peptides in hemocytes and hematopoietic tissue from freshwater crayfish *Pacifastacus leniusculus*: characterization and expression pattern. Dev. Comp. Immunol. 31, 441–455.

Jiravanichpaisal, P., Söderhäll, K., Söderhäll, I., 2010. Inflammation in arthropods. Curr. Pharmaceut. Des. 16, 4166–4174.

Kagan, B.L., Ganz, T., Lehrer, R.I., 1994. Defensins: a family of antimicrobial and cytotoxic peptides. Toxicology 87, 131–149.

Khalturin, K., Hemmrich, G., Fraune, S., Augustin, R., Bosch, T.C.G., 2009. More than just orphans: are taxonomically-restricted genes important in evolution? Trends Genet. 25, 404–413.

Kibbe, W.A., 2007. OligoCalc: an online oligonucleotide properties calculator. Nucleic Acids Res. 35, W43–W46.

Knappe, D., Piantavigna, S., Hansen, A., Mechler, A., Binas, A., Nolte, O., Martin, L.L., Hoffmann, R., 2010. Oncocin (VDKPPYLPRPRPPRRIYNR-NH_2): a novel antibacterial peptide optimized against gram-negative human pathogens. J. Med. Chem. 5240–5247.

Kuipers, B.J.H., Gruppen, H., 2007. Prediction of molar extinction coefficients of proteins and peptides using UV absorption of the constituent amino acids at 214 nm to enable quantitative reverse phase high-performance liquid Chromatography – Mass

spectrometry analysis. J. Agric. Food Chem. 55, 5445–5451.
Lee, S.Y., Lee, B.L., Söderhäll, K., 2003. Processing of an antibacterial peptide from hemocyanin of the freshwater crayfish *Pacifastacus leniusculus*. J. Biol. Chem. 278, 7927–7933.
Leoni, G., De Poli, A., Mardirossian, M., Gambato, S., Florian, F., Venier, P., Wilson, D., Tossi, A., Pallavicini, A., Gerdol, M., 2017. Myticalins: a novel multigenic family of linear, cationic antimicrobial peptides from marine mussels (Mytilus spp.). Mar. Drugs 15, 23.
Liu, H., Jiravanichpaisal, P., Cerenius, L., Lee, B.L., Söderhäll, I., Söderhäll, K., 2007. Phenoloxidase is an important component of the defense against *Aeromonas hydrophila* infection in a Crustacean, *Pacifastacus leniusculus*. J. Biol. Chem. 282, 33593–33598.
Lodge, D.M., Deines, A., Gherardi, F., Yeo, D.C.Y., Arcella, T., Baldridge, A.K., Barnes, M.A., Chadderton, W.L., Feder, J.L., Gantz, C.A., Howard, G.W., Jerde, C.L., Peters, B.W., Peters, J.A., Sargent, L.W., Turner, C.R., Wittmann, M.E., Zeng, Y., 2012. Global introductions of crayfishes: evaluating the impact of species invasions on ecosystem services. Annu. Rev. Ecol. Evol. Syst. 43, 449–472.
Manfrin, C., Peruzza, L., Bonzi, L., Pallavicini, A., Giulianini, P., 2015. Silencing two main isoforms of crustacean hyperglycemic hormone (CHH) induces compensatory expression of two CHH-like transcripts in the red swamp crayfish *Procambarus clarkii*. Invertebr. Surviv. J. 12, 29–37.
Mardirossian, M., Grzela, R., Giglione, C., Meinnel, T., Gennaro, R., Mergaert, P., Scocchi, M., 2014. The host antimicrobial peptide Bac71-35 Binds to bacterial ribosomal proteins and inhibits protein synthesis. Chem. Biol. 21, 1639–1647.
Mardirossian, M., Pérébaskine, N., Benincasa, M., Gambato, S., Hofmann, S., Huter, P., Müller, C., Hilpert, K., Innis, C.A., Tossi, A., Wilson, D.N., 2018. The dolphin proline-rich antimicrobial peptide Tur1A inhibits protein synthesis by targeting the bacterial ribosome. Cell Chem. Biol. 25, 530–539.
McGrath, L.L., Vollmer, S.V., Kaluziak, S.T., Ayers, J., 2016. De novo transcriptome assembly for the lobster *Homarus americanus* and characterization of differential gene expression across nervous system tissues. BMC Genomics 17.
Otvos, L.J., 2000. Antibacterial peptides isolated from insects. J. Pept. Sci. 6, 497–511.
Otvos, L.J., 2002. The short proline-rich antibacterial peptide family. Cell. Mol. Life Sci. 59, 1138–1150.
Paulsen, V.S., Mardirossian, M., Blencke, H.M., Benincasa, M., Runti, G., Nepa, M., Haug, T., Stensvåg, K., Scocchi, M., 2016. Inner membrane proteins YgdD and SbmA are required for the complete susceptibility of Escherichia coli to the proline-rich antimicrobial peptide arasin. Microbiology 1 (1–25), 601–609.
Petersen, T.N., Brunak, S., Von Heijne, G., Nielsen, H., 2011. SignalP 4.0: discriminating signal peptides from transmembrane regions. Nat. Methods 8, 785–786.
Reese, M.G., Eeckman, F.H., Kulp, D., Haussler, D., 1997. Improved splice site detection in Genie. J. Comput. Biol. 4, 311–323.
Rice, P., Longden, I., Bleasby, A., 2000. EMBOSS: the European molecular Biology open software suite. Trends Genet. 16, 276–277.
Rončević, T., Gajski, G., Ilić, N., Goić-Barišić, I., Tonkić, M., Zoranić, L., Simunić, J., Benincasa, M., Mijaković, M., Tossi, A., Juretić, D., 2017. PGLa-H tandem-repeat peptides active against multidrug resistant clinical bacterial isolates. Biochim. Biophys. Acta BBA - Biomembr. 1859, 228–237.
Rotllant, G., Nguyen, T.V., Sbragaglia, V., Rahi, L., Dudley, K.J., Hurwood, D., Ventura, T., Company, J.B., Chand, V., Aguzzi, J., Mather, P.B., 2017. Sex and tissue specific gene expression patterns identified following de novo transcriptomic analysis of the Norway lobster, *Nephrops norvegicus*. BMC Genomics 18.
Runti, G., Ruiz, M.d.C.L., Stoilova, T., Hussain, R., Jennions, M., Choudhury, H.G., Benincasa, M., Gennaro, R., Beis, K., Scocchi, M., 2013. Functional characterization of SbmA, a bacterial inner membrane transporter required for importing the line-rich antibacterial peptide, with sequence similarity to bactenecin-7, from the haemocytes of the shore crab, *Carcinus maenas*. Eur. J. Biochem. 240, 532–539.
Scocchi, M., Tossi, A., Gennaro, R., 2011. Proline-rich antimicrobial peptides: converging to a non-lytic mechanism of action. Cell. Mol. Life Sci. 68, 2317–2330.
Shi, X.Z., Li, X.C., Wang, S., Zhao, X.F., Wang, J.X., 2010. Transcriptome analysis of hemocytes and hepatopancreas in red swamp crayfish, *Procambarus clarkii,* challenged with white spot syndrome virus. Invertebr. Surviv. J. 7, 119–131.
Shi, X.Z., Zhao, X.F., Wang, J.X., 2014. A new type antimicrobial peptide astacidin functions in antibacterial immune response in red swamp crayfish *Procambarus clarkii*. Dev. Comp. Immunol. 43, 121–128.
Simunić, J., Petrov, D., Bouceba, T., Kamech, N., Benincasa, M., Juretić, D., 2014. Trichoplaxin - a new membrane-active antimicrobial peptide from placozoan cDNA. Biochim. Biophys. Acta BBA - Biomembr. 1838, 1430–1438.
Stacchini, A., Aragno, M., Vallario, A., Alfarano, A., Circosta, P., Gottardi, D., Faldella, A., Rege-Cambrin, G., Thunberg, U., Nilsson, K., 1999. MEC1 and MEC2: two new cell lines derived from B-chronic lymphocytic leukaemia in prolymphocytoid transformation. Leuk. Res. 23, 127–136.
Steiner, H., Hultmark, D., Engström, Å., Bennich, H., Boman, H.G., 1981. Sequence and specificity of two antibacterial proteins involved in insect immunity. Nature 292, 246–248.
Tan, M.H., Gan, H.M., Gan, H.Y., Lee, Y.P., Croft, L.J., Schultz, M.B., Miller, A.D., Austin, C.M., 2016. First comprehensive multi-tissue transcriptome of *Cherax quadricarinatus* (Decapoda: Parastacidae) reveals unexpected diversity of endogenous cellulase. Org. Divers. Evol. 16, 185–200.
Tessera, V., Guida, F., Juretić, D., Tossi, A., 2012. Identification of antimicrobial peptides from teleosts and anurans in expressed sequence tag databases using conserved signal sequences. FEBS J. 279, 724–736.
Theissinger, K., Falckenhayn, C., Blande, D., Toljamo, A., Gutekunst, J., Makkonen, J., Jussila, J., Lyko, F., Schrimpf, A., Schulz, R., Kokko, H., 2016. De Novo assembly and annotation of the freshwater crayfish *Astacus astacus* transcriptome. Mar. Genomics 28, 7–10.
Tom, M., Manfrin, C., Mosco, A., Gerdol, M., Moro, G.D.M.D., Pallavicini, A., Giulianini, P.G., 2014. Different transcription regulation routes are exerted by L- and D-amino acid enantiomers of peptide hormones. J. Exp. Biol. 217, 4337–4346.
Tossi, A., Sandri, L., Giangaspero, A., 2000. Amphipathic, α-helical antimicrobial peptides. Pept. Sci. 55.
Untergrasser, A., Cutcutache, I., Koressaar, T., Ye, J., Faircloth, B.C., Remm, M., Rozen, S.G., 2012. Primer3 - new capabilities and interfaces. Nucleic Acids Res. 40, e115.
Wu, B., Zhang, C., Qin, X., Shi, L., Zhao, M., 2019. Identification and function of penaeidin 3 and penaeidin 5 in *Fenneropenaeus merguiensis*. Fish Shellfish Immunol. 89, 623–631.
Wu, L., Zhou, Y., Abbas, M.N., Kausar, S., Chen, Q., Jiang, C.X., Dai, L.S., 2017. Molecular structure and functional characterization of the peroxiredoxin 5 in *Procambarus clarkii* following LPS and Poly I:C challenge. Fish Shellfish Immunol. 71, 28–34.
Zasloff, M., 2002. Antimicrobial peptides of multicellular organisms. Nature 415, 389–395.
Zhou, M., Abbas, M.N., Kausar, S., Jiang, C.X., Dai, L.S., 2017. Transcriptome profiling of red swamp crayfish (*Procambarus clarkii*) hepatopancreas in response to lipopolysaccharide (LPS) infection. Fish Shellfish Immunol. 71, 423–433.
Zhu, J.J., Ye, Z.Z., Li, C.S., Kausar, S., Abbas, M.N., Xiang, G.H., Qian, X.Y., Dai, L.S., 2019. Identification and molecular characterization of a novel anti-lipopolysaccharide factor (ALF) from red swamp crayfish, *Procambarus clarkii*. Biol. Macromol. 132, 43–50.